Development 133, 3919-3928 (2006) doi:10.1242/dev.02538

Man1, an inner nuclear membrane protein, regulates vascular remodeling by modulating transforming growth factor β signaling

Akihiko Ishimura[1], Jennifer K. Ng[2], Masanori Taira[3], Stephen G. Young[4] and Shin-Ichi Osada[1,*]

A growing number of integral inner nuclear membrane (INM) proteins have been implicated in diverse cellular functions. Man1, an INM protein, has recently been shown to regulate transforming growth factor (Tgf) β superfamily signaling by interacting with receptor-associated Smads. However, the in vivo roles of Man1 have not been fully characterized. Here, we show that Man1 regulates vascular remodeling by analyzing *Man1*-deficient embryos lacking the Smad interacting domain. *Man1*-deficient embryos die at midgestation because of defects in embryonic vasculature; the primary capillary plexus forms, but subsequent remodeling is perturbed. It has been proposed that the angiogenesis process is divided into two balanced phases, the activation and resolution/maturation phases, both of which are regulated by Tgfβ1. We have demonstrated, in *Man1*-deficient embryos, the expression of *Tgfb1* is upregulated and Smad2/3 signaling is abnormally activated, resulting in increased extracellular matrix deposition, a hallmark of the resolution phase of angiogenesis. We have also showed that the recruitment of mural cells to the vascular wall is severely disturbed in mutants, which may lead to disruption of intercellular communication between endothelial and mural cells required for proper vascular remodeling. These results have revealed a novel role for Man1 in angiogenesis and provide the first evidence that vascular remodeling can be regulated at the INM through the interaction between Man1 and Smads.

KEY WORDS: Man1 (Lemd3), Inner nuclear membrane protein, Transforming growth factor β signaling, Smad, Angiogenesis, Vascular remodeling, *Xenopus*, Mouse

INTRODUCTION

The nuclear envelope (NE) is composed of outer and inner nuclear membranes (INM), nuclear lamina and nuclear pore complexes. The outer nuclear membrane is directly continuous with the endoplasmic reticulum membrane, whereas the INM is lined by a nuclear lamina network formed mainly by type V intermediate filaments containing type A and type B lamins. The nuclear lamins bind to several INM proteins, including lamina-associated polypeptides 1 and 2β (LAP1, LAP2β), emerin and Man1 (Lemd3 – Mouse Genome Informatics; the subject of this study), which share a common structural motif of about 40 amino acid residues, called the LEM (LAPs, emerin and Man1) domain (Lin et al., 2000). The nuclear lamins and the LEM domain proteins interact with barrier-to-autointegration factor, through which they are involved in higher-order chromatin organization, nuclear assembly and gene regulation (Gruenbaum et al., 2005). However, the functions of a large number of putative integral NE proteins remain to be elucidated (Schirmer et al., 2003).

Human MAN1 was originally identified as one of three antigens recognized by autoantibodies from an individual with a collagen vascular disease (Lin et al., 2000). Man1 has a N-terminal LEM domain, two putative transmembrane domains, a Man1-SRC1P C-terminal domain of unknown function (Mans et al., 2004) and an RNA recognition motif. An RNA interference-mediated loss-of-function experiment with the Man1 ortholog in *C. elegans*, Ce-MAN1, provides evidence that Ce-MAN1, in combination with Ce-emerin, plays an essential role in chromosome segregation and cell division (Liu et al., 2003).

The linkage between the INM and growth factor-related signal transduction was initially discovered by analyzing the roles of XMAN1 and SANE (Smad1 antagonistic effector), both of which are *Xenopus* orthologs of Man1, in early embryogenesis (Osada et al., 2003; Raju et al., 2003). We identified XMAN1 as a novel factor that neuralizes the ectoderm and dorsalizes the ventral mesoderm. In *Xenopus*, inhibition of the bone morphogenetic protein (Bmp) pathway is a crucial step for neural induction (Harland, 2000). We have demonstrated that XMAN1 antagonizes the Bmp pathway by interacting with the MH2 domain of the receptor-associated Smads (R-Smads) that mediate Bmp signaling (Smad1, Smad5 and Smad8) through its C-terminal region. SANE was isolated as a novel Smad1-interacting protein by the yeast two-hybrid system and shows essentially the same activities as XMAN1.

Abnormal function of the NE is implicated in a wide range of human diseases, collectively termed laminopathies (Burke and Stewart, 2002). Heterozygous loss-of-function mutations in human *MAN1* (*LEMD3* – Human Gene Nomenclature Database) cause osteopoikilosis, Buschke-Ollendorf syndrome and melorheostosis (Hellemans et al., 2004), all of which are characterized by hyperostotic bones. The associated mutations involve the deletion of the C-terminal region of MAN1, which is the interaction domain for R-Smads. Interestingly, expression of wild-type human LEMD3 in mammalian cells suppresses both transforming growth factor (TGF) β1-dependent and BMP-dependent reporter activation, whereas expression of a mutant MAN1 with either of the *LEMD3* mutations

[1]The 21st Century Center of Excellence Program, Akita University School of Medicine, Hondo 1-1-1, Akita, Akita 010-8543, Japan. [2]The J. David Gladstone Institutes, 1650 Owen Street, San Francisco, CA94158, USA. [3]Department of Biological Sciences, Graduate School of Science, University of Tokyo, Hongo 7-3-1, Bunkyo-ku, Tokyo 113-0033, Japan. [4]Department of Medicine and Human Genetics, David Geffen School of Medicine, University of California at Los Angeles, 650 Charles E. Young Dr South, 47-123 CHS, Los Angeles, CA 90095, USA.

*Author for correspondence (e-mail: osada@med.akita-u.ac.jp)

Accepted 18 July 2006

is unable to suppress TGFβ1 signaling. These observations indicate that human MAN1 antagonizes both the BMP- and TGFβ/activin-signaling pathways, a conclusion that was also demonstrated independently by two other groups using mammalian cells (Lin et al., 2005; Pan et al., 2005). Thus, increased bone density and disseminated connective tissue nevi found in individuals with the *LEMD3* mutations and elevated elastin production in fibroblasts from patients with Buschke-Ollendorf syndrome (Giro et al., 1992) might be explained by augmented sensitivity to the bone-forming activity of BMPs and the extracellular matrix-producing activity of TGFβ1.

In this study, to better understand the role of Man1 in cellular and developmental processes, we analyzed the consequence of Man1 deficiency in vivo. We used gene trapping to generate *Man1*-deficient mice, in which the C-terminal region containing the Smad-interaction domain was deleted. We found that the angiogenesis processes required to build a mature capillary were severely perturbed in *Man1*-deficient embryos. These embryos had an abnormal augmentation of Smad2/3 signaling, resulting in increased extracellular matrix deposition, which is believed to inhibit endothelial cell proliferation and migration (Pepper, 1997). These results provide the first evidence that Man1 plays a crucial role in angiogenesis, acting as a 'gatekeeper' at the INM to modulate the activity of the Tgfβ signaling pathway through the interaction with receptor-associated Smads.

MATERIALS AND METHODS

Xenopus embryo manipulation

Artificial fertilization, culture of embryonic tissues and embryo staging were performed as previously described (Kay and Peng, 1991; Nieuwkoop and Faber, 1967). Whole-mount in situ hybridization of *Xenopus* embryos was performed. RT-PCR and luciferase assays using ectodermal explants were carried out as previously described (Osada et al., 2003).

Generation of *Man1*-deficient mice

A mouse embryonic stem cell line (cell line XST167, strain 129/Ola) containing an insertional mutation in *Man1* was created in a gene-trapping program by BayGenomics (http://baygenomics.ucsf.edu/). The gene-trapping vector, pGT1Mpfs, was designed to create an in-frame fusion between the 5′ exons of the trapped gene and a reporter gene, *βgeo*. The ES cells were injected into C57BL/6J blastocysts to create chimeric mice, which bred to generate heterozygous *Man1*-deficient ($Man1^{+/\Delta}$) mice. Mouse embryonic fibroblasts (MEFs) were established from embryonic day (E) 16.5 wild-type and $Man1^{+/\Delta}$ embryos using standard procedures (Nagy et al., 2003).

Genotypes of embryos older than E9.5 were determined by Southern blotting. Genomic DNA isolated from tails, yolk sacs and embryos were digested with *Pst*I and hybridized with a *Man1* probe located upstream of the insertion site. The probe was amplified from mouse genomic DNA with primers 5′-GCGCTGGGTTACTTTGTGTGCTG-3′ and 5′-GCTTCCCG-TTCACCACACTTCTG-3′. Signals were visualized with the Gene Image Random-Prime Labeling and Detection System (Amersham).

RT-PCR

Genotypes of embryos from E7.0-E9.0 and gene expression profiles of wild-type and mutant embryos were analyzed by RT-PCR. Total RNA was isolated from yolk sacs, ectoplacental cones and embryos with the High Pure RNA Tissue Isolation kit (Roche). First-strand cDNA was synthesized with Superscript Reverse Transcriptase (RT) III (Invitrogen). Primer sequences and PCR conditions are presented in Table 1.

Whole-mount in situ hybridization

Whole-mount in situ hybridization of mouse embryos was performed as described previously (Yamaguchi et al., 1993) with the exception that hybridization was performed at 70°C. Digoxygenin (DIG)-labeled antisense RNA probes were synthesized with the DIG RNA Labeling mix (Roche).

X-gal staining and immunohistochemistry

X-gal staining of heterozygous embryos was performed using standard procedures (Nagy et al., 2003). For whole-mount immunohistochemistry, E9.5 yolk sacs and embryos were fixed in 4% paraformaldehyde (PFA) in phosphate-buffered saline followed by dehydration. After blocking, the specimens were incubated with an anti-Pecam-1 antibody (MEC13.3; BD Pharmingen; 1:400) and then treated with a horseradish peroxidase (HRP)-coupled anti-rat IgG antibody (Biosource, 1:500) as a secondary antibody. The signals were detected with 0.3 mg/ml 3,3′-diaminobenzidine (DAB) containing 0.8 mg/ml nickel chloride.

For section immunohistochemistry, dissected embryos were fixed in 4% PFA, dehydrated, embedded in paraffin and sectioned. Antibodies to smooth muscle α-actin (1A4; Dako; 1:500), phospho-histone H3 (Sigma; 1:2000), activated caspase 3 (1:2000), or ssDNA (Dako; 1:400) were used as primary antibodies. Vecta stain Elite peroxidase kit (Vector) and the ImmunoPure Metal Enhanced DAB Substrate kit (Pierce) were used for visualization

For immunofluorescence assays, paraffin-embedded sections were treated with the following primary antibodies: anti-fibronectin (Sigma; 1:300), anti-phospho-Smad1/5/8 (Cell Signaling; 1:100) and anti-phospho-Smad2 (Cell Signaling; 1:500). After washing, the sections were incubated with an Alexa 546-conjugated anti-rabbit IgG antibody (Invitrogen; 1:2000). Nuclei were visualized with 4,6-diamidino-2-phenylindole (DAPI). Images were obtained using a confocal microscope (model LSM 510; Carl Zeiss).

Transmission electron microscopy

E9.5 embryos were fixed with 3% glutaraldehyde in 0.1 M sodium cacodylate buffer at pH 7.4 and post-fixed with 1% osmium tetroxide in the same buffer. After dehydration, they were substituted by propylene oxide and embedded in epoxy resin. Ultrathin sections were doubly stained with uranyl acetate and lead citrate, and examined with an H-7650 transmission electron microscope (Hitachi).

Table 1. RT-PCR primer pairs used in this study

Gene	Primers (5′ to 3′)	Product (bp)	Annealing temperature (°C)/cycles
β-Actin	F, TGGCACCACACCTTCTACAATGAGC; R, GCACAGCTTCTCCTTAATGTCACCCGC	395	62/32
βgeo	F, TTATCGATGAGCGTGGTGGTTATGC; R, GCGCGTACATCGGGCAAATAATATC	681	56/35
Fibronectin 1	F, GGACAACTTCTGGTCCTCTCC; R, GTTGCCTAGGTAGGTCCGTTC	356	60/28
Id1	F, GATCATGAAGGTCGCCAGTG; R, TCCATCTGGTCCCTCAGTGC	476	60/31
Man1 (exons 4-5)	F, GGAGTTTCAGCGCTCACTA; R, TGGGAACAAACGGCGGATTGACC	377	56/35
Man1-βgeo	F, GGAGTTTCAGCGCTCACTA; R, TCACAGCCACAGTCCGGCAG	1420	56/30
Cdkn1a	F, AGCCTGAAGACTGTGATGGG; R, AAAGTTCCACCGTTCTCGG	228	62/35
Serpine1	F, ACAGTGGGAAGAGACGCCTTC; R, GGTGGGCAAGGTGGACATTTC	462	60/33
Tagln	F, GCTACTCTCCTTCCAGTCCACAAACGACCA; R, CCTTCCCTTTCTAACTGATGATCTG	664	60/28
Acta2	F, GGCATCCACGAAACCACCTA; R, CACGAGTAACAAATCAAAGC	419	60/24
Smad7	F, TCCTGCTGTGCAAAGTGTTC; R, AGTAAGGAGGAGGGGGAGAC	165	60/34
Tgfb1	F, GCTGCGCTTGCAGAGATTAAA; R, TTGCTGTACTGTGTGTCCAG	552	56/33

F, forward; R, reverse.

Western blotting

E9.5 embryos were dissected out and yolk sacs were removed for genotyping. Dissected embryos and MEFs were lysed in modified RIPA buffer (50 mM Tris-HCl at pH 7.4, 150 mM NaCl, 1% NP-40, 0.5% sodium deoxycholate, 1 mM EDTA supplemented with phosphatase and protease inhibitors). Lysates were cleared by centrifugation and quantitated with the BCA Protein Assay Kit (PIERCE). The lysates (20 μg) were separated on a 5-10% gradient gel (BioRad). The following primary antibodies were used: anti-β-galactosidase (Promega; 1:1000), anti-N-terminal human MAN1 (Santa Cruz Biotechnology; 1:200), anti-fibronectin (Sigma; 1:1000) and anti-β-tubulin (Sigma; 1:5000).

RESULTS

XMAN1 regulates activin/nodal signaling in *Xenopus* embryos

Although recent cell culture data indicate that Man1 inhibits Tgfβ1 signaling in mammalian cells by interacting with the Tgfβ1/activin-responsive Smad proteins Smad2 and Smad3 (Hellemans et al., 2004; Lin et al., 2005; Pan et al., 2005), it is not clear whether this is also the case in vivo. To address this, we first examined whether a *Xenopus* ortholog of MAN1, XMAN1, inhibits activin/nodal signaling during *Xenopus* development. Chordin is expressed in the Spemann organizer at the early gastrula stages and is a downstream target for activin/nodal signaling (Sasai et al., 1994). When *XMAN1* mRNA was injected into the future organizer region, the expression of *chordin* was almost completely suppressed (Fig. 1A). Conversely, delivery of the antisense morpholino oligonucleotides (MO), which specifically inhibit XMAN1 functions in vivo (Osada et al., 2003), caused a large expansion of the expression domain for *chordin*, whereas it was unchanged in embryos injected with four-base-mismatched MO.

The above results were supported by animal cap (ectodermal explant) assays. *Xenopus* nodal-related factor 1 (Xnr1) induced mesodermal markers (*Xbra*, *chordin* and *goosecoid*) in animal caps as previously described (Jones et al., 1995). Wild-type XMAN1 and the C-terminal fragment of XMAN1 (XMAN1-CT) containing the Smad-interacting domain, suppressed the induction of these markers by Xnr1, but a mutant lacking the CT (XMAN1-ΔCT) did not (Fig. 1B).

Xnr1 expression is autoregulated through an activin/nodal response element composed of three Foxh1 (FAST-1)-binding sites present in the first intron (Osada et al., 2000). We performed a reporter assay with a luciferase construct (Int1) containing this element to study whether XMAN1 inhibits Xnr1-dependent transcription. As shown in Fig. 1C, the activation of Xnr1-dependent Int1 was suppressed by XMAN1 and XMAN1-CT, but not by XMAN1-ΔCT. We also found that XMAN1 could directly bind to Smad2 and Smad3 via its C-terminal region (Osada et al., 2003) (data not shown) in the *Xenopus* embryo, consistent with the works using cultured cells (Hellemans et al., 2004; Lin et al., 2005; Pan et al., 2005). These data indicate that XMAN1 negatively regulates activin/nodal signaling in addition to Bmp signaling in vivo.

Generation of *Man1*-deficient mice

Although Man1 loss-of-function analyses have been performed in *C. elegans* (Liu et al., 2003), *Xenopus* (Osada et al., 2003) and cultured mammalian cells (Hellemans et al., 2004; Pan et al., 2005), the consequence of the complete loss of functional Man1 in whole organisms is unknown, even in human disease states. To obtain insights into the requirement for Man1 in mammalian development and cellular functions, we generated *Man1*-deficient mice using an embryonic stem cell line in which *Man1* had been disrupted by gene trapping. A DNA sequence tag generated by 5′ rapid amplification of cDNA ends analysis revealed that the insertional mutation in *Man1* occurred in intron 4 (Fig. 2A). Embryos were genotyped by

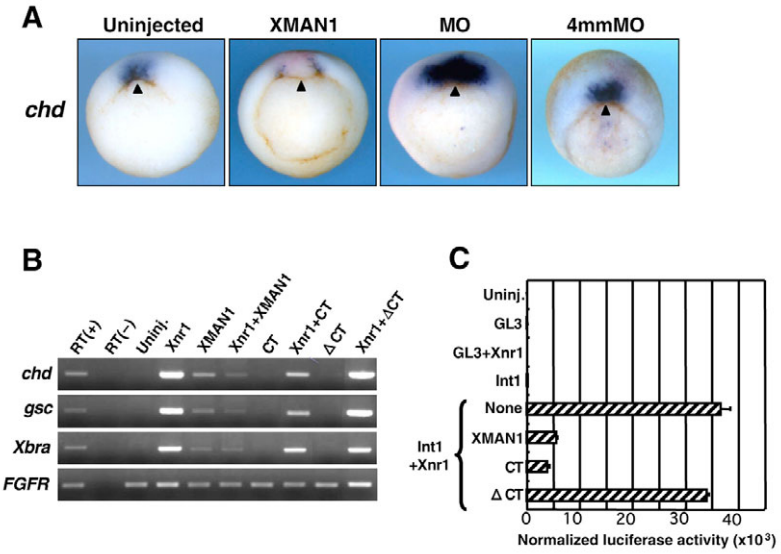

Fig. 1. XMAN1 inhibits the activin/nodal pathway in the *Xenopus* embryo. (**A**) Whole-mount in situ hybridization for *chordin* (*chd*) at stage 10.5. MO, antisense morpholino oligonucleotides against XMAN1; 4mmMO, four-base-mismatched MO. *XMAN1* mRNA (1 ng/embryo) or MO (75 ng/embryo) was injected into two dorsal blastomeres at the four-cell stage. Arrowheads indicate the dorsal lip. (**B**) Suppression of Xnr1-dependent mesodermal induction by XMAN1. RT-PCR of animal caps for *chd* and *goosecoid* (*gsc*), dorsal mesoderm markers and *Xenopus brachyury* (*Xbra*), a pan-mesodermal marker, at the equivalent of stage 10.5. *Xnr1* mRNA (100 pg/embryo) and either mRNA for XMAN1 (2 ng/embryo), C-terminal (CT)-XMAN1 (500 pg/embryo, equivalent amount in mol to XMAN1) or CT-truncated (ΔCT)-XMAN1 (1500 pg/embryo, equivalent amount in mol to XMAN1) were injected. *FGFR* is the loading control. (**C**) Suppression of activin/nodal-dependent *Xnr1* intron1-luciferase (Int1) activation by XMAN1 constructs. A control of GL3-luciferase or an Int1 construct (100 pg/embryo) was injected together with a *Renilla* luciferase plasmid (2 pg/embryo), *Xnr1* mRNA (100 pg/embryo) and mRNA for XMAN1 (1 ng/embryo), CT (250 pg/embryo) or ΔCT (750 pg/embryo).

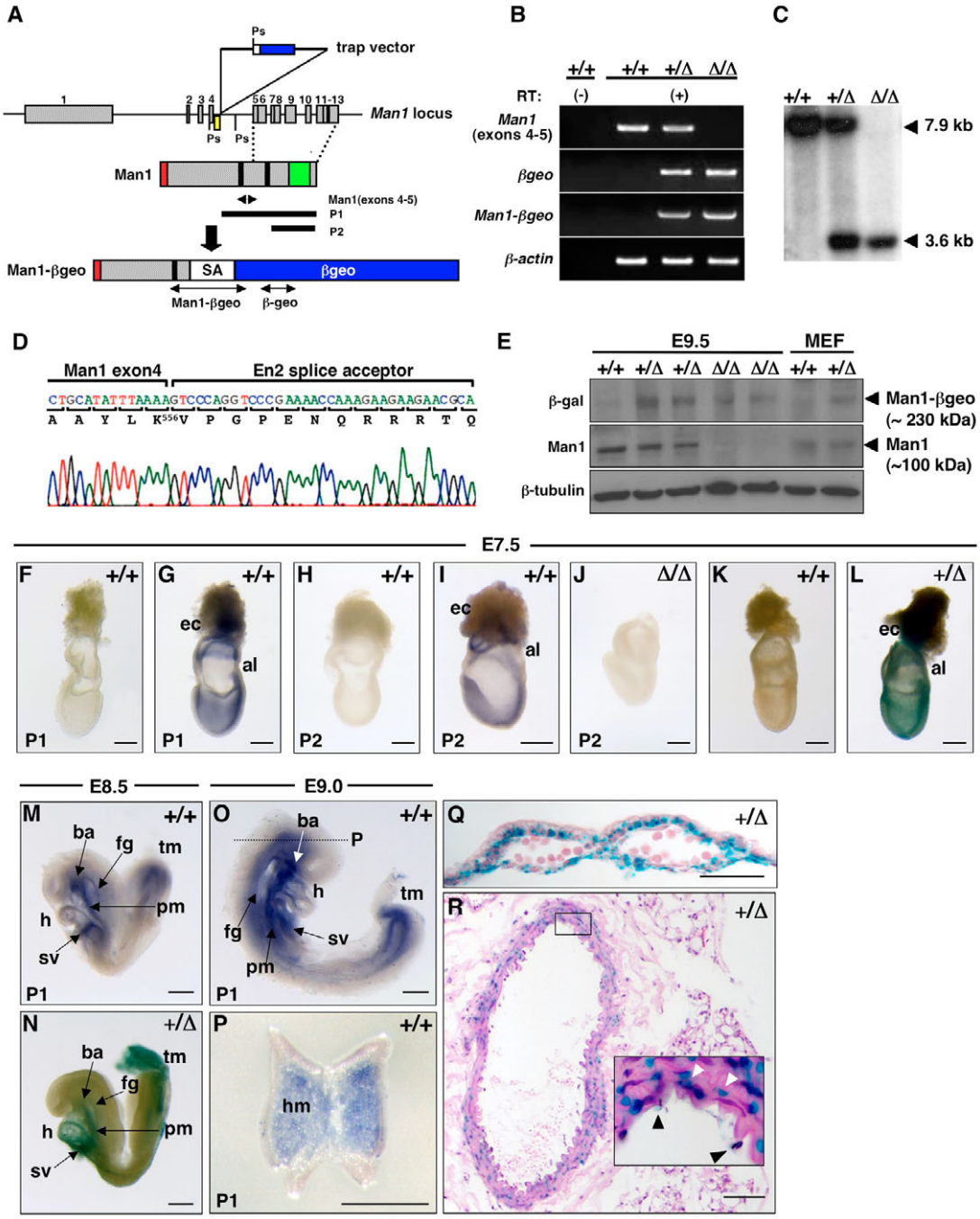

Fig. 2. Generation of *Man1*-deficient mice and developmental expression of *Man1*. (**A**) The exon-intron organization of *Man1* with the genetrap vector (upper) and a schematic structure of Man1 (middle) are depicted. The LEM domain (red), transmembrane domains (black) and the Smad-interacting domain (green) are indicated. The genetrap vector, which contains an engrailed 2 splice acceptor (SA, white) and *βgeo* (blue), was inserted in intron 4 to produce a Man1-*βgeo* fusion protein (lower) lacking the *C*-terminal region containing the Smad-interacting domain. Numbers indicate exons. Genomic DNA was digested with *Pst*I (Ps) for Southern blotting using a probe (yellow) outside the insertion site. P1 and P2 are probes for whole-mount in situ hybridization analysis. Double-headed arrows indicate the positions of the cDNA fragments amplified by RT-PCR in B. (**B**) Genotyping by RT-PCR using yolk sacs from embryos at E8.5. (**C**) Genotyping by Southern blotting of tail DNA from embryos at E9.5. The wild-type allele yielded a 7.9 kb band and the mutant allele yielded a 3.6 kb band. (**D**) A sequencing result of the *Man1-βgeo* transcript shown in B. Three other independent clones showed the same results. The deduced amino acid sequence is shown. (**E**) Western blot of lysates from E9.5 embryos and MEFs with antibodies to β-galactosidase and Man1. β-Tubulin was used as a loading control. (**F-J**,**M**,**O**,**P**) Whole-mount in situ hybridization with the sense (F,H) or antisense (G,I,J,M,O,P) P1 and P2 probes. No signals were observed in the mutant embryo probed with the antisense P2 probe (J). (P) A cryosection of the E9.0 embryo shown in O. Anterior to the left in F-O. Whole-mount X-gal staining in wild-type (**K**) and *Man1*$^{+/\Delta}$ (**L**,**N**,**Q**,**R**) embryos and mice. (Q) A section through the yolk sac at E9.5. (R) The dorsal aorta of an 11-week-old mouse. In the inset, black arrowheads indicate endothelial cells; white arrowheads indicate VSMCs. Genotypes of the embryos and stages are indicated. al, allantois; ba, branchial arch; ec, ectoplacental cone; fg, foregut; h, heart; hm, head mesenchyme; pm, paraxial mesoderm; sv, sinus venosus; tm, tail mesenchyme. Scale bars: 200 μm in F-P; 50 μm in Q,R.

RT-PCR at E7.0-E9.0 with *Man1* and *βgeo* primer pairs (Fig. 2B) and by Southern blots at E9.5 and later with a probe located upstream of the insertion site (Fig. 2C). We amplified a fusion transcript composed of the fourth exon of *Man1*, an *Engrailed-2* splice acceptor and full-length *βgeo* from *Man1*-deficient embryos (Fig. 2D). The deduced gene product of this transcript indicates that a Man1-βgeo fusion protein lacking the *C*-terminal Smad-interacting domain was generated in *Man1*-deficient embryos. We refer to the genetrap allele as *Man1*Δ hereafter.

We determined whether any wild-type Man1 protein was made from the genetrap allele by western blotting. An antibody to Man1 recognized a ~100 kDa band, which was comparable with exogenously overexpressed human MAN1 (not shown), in lysates prepared from wild-type and $Man1^{+/\Delta}$ embryos and MEFs, but not in those from $Man1^{\Delta/\Delta}$ embryos (Fig. 2E). Conversely, a band of ~230 kDa corresponding to the predicted Man1-βgeo fusion protein was detected by an antibody to β-galactosidase in the $Man1^{+/\Delta}$ and $Man1^{\Delta/\Delta}$ specimens, but not in the wild-type ones. Thus, the Man1-βgeo fusion protein in $Man1^{\Delta/\Delta}$ embryos is unlikely to retain regulatory activity on Smad signaling.

We analyzed the temporal and spatial expression domains for Man1 during early embryogenesis by whole-mount X-gal staining in $Man1^{+/\Delta}$ embryos. *lacZ* expression was detected in the epiblast, the allantois and the ectoplacental cone at E7.5 (Fig. 2L), and in the heart, the branchial arches, the foregut, the paraxial mesoderm, the sinus venosus and the tail mesenchyme at E8.5 (Fig. 2N). No signals were detected in a wild-type littermate embryo (Fig. 2K). As for the vascular system, *lacZ* was detected in visceral endodermal, mesodermal and endothelial cells in the yolk sac (Fig. 2Q), and endothelial and vascular smooth muscle cells (VSMCs) in the dorsal aorta (Fig. 2R). *lacZ* was also observed in a wide range of tissue/cell populations in the adult (see Fig. S1 in the supplementary material). These *lacZ*-positive tissues correspond well to the localization of *Man1* transcripts (Fig. 2F-J,M,O), suggesting that the βgeo gene was under the control of endogenous *Man1* promoter. *Man1* is also strongly expressed in the head mesenchyme at E9.0 (Fig. 2P). An antisense probe specifically hybridizes to the sequence covering the C-terminal region (P2) gave no signals in $Man1^{\Delta/\Delta}$ embryos (Fig. 2J), supporting further that the *C*-terminal transcript was not expressed in $Man1^{\Delta/\Delta}$ embryos.

Man1 deficiency causes embryonic lethality

$Man1^{+/\Delta}$ mice are normal in terms of growth, fertility and lifespan. Although humans with heterozygous *LEMD3* mutations exhibit prominent bone and connective tissue phenotypes (Hellemans et al., 2004), we did not detect any abnormalities in bone density by magnetic resonance imaging or connective tissue nevi by skin histology in $Man1^{+/\Delta}$ mice (data not shown). No homozygous mice ($Man1^{\Delta/\Delta}$) were recovered at weaning. To elucidate further the apparent embryonic lethal phenotype, we analyzed the offspring of heterozygote intercrosses at various stages of development. Although $Man1^{\Delta/\Delta}$ embryos at E7.5, E8.5, E9.5 and E10.5 were recovered at the predicted mendelian frequencies (see Table S1 in the supplementary material), the number of $Man1^{\Delta/\Delta}$ embryos at E11.5 was lower than predicted. No homozygous mutants were recovered at E12.5 or later; thus, $Man1^{\Delta/\Delta}$ embryos died at about E10.5-E11.5.

Nodal expression is deregulated in *Man1*-deficient embryos

Members of the TGFβ superfamily play a crucial role in mesoderm formation and patterning of the embryo (Chang et al., 2002; Whitman, 1998). We first examined the possibility that $Man1^{\Delta/\Delta}$ embryos die from impaired mesoderm formation by performing whole-mount in situ hybridization. Because $Man1^{\Delta/\Delta}$ embryos showed a 0.5- to 1.0-day delay in development, we compared the mutant embryos with stage-matched wild-type embryos. We found no obvious differences in the expression domains for the mesodermal markers *Nodal* (Fig. 3A; $^{+/+}$, n=6; $^{\Delta/\Delta}$, n=4), chordin (Fig. 3B; $^{+/+}$, n=7; $^{\Delta/\Delta}$, n=4), *Bmp4* (Fig. 3C; $^{+/+}$, n=5; $^{\Delta/\Delta}$, n=5) and brachyury (Fig. 3E; $^{+/+}$, n=2; $^{\Delta/\Delta}$, n=3), between the wild-type and mutant embryos, although we observed consistently stronger intensity of expression of *Nodal* and chordin in the mutants. *Nodal* normally shows an asymmetric expression in the left lateral plate mesoderm (LPM) at E8.25 (Lowe et al., 1996). However, in the mutant embryos, *Nodal* was ectopically expressed in the right LPM (Fig. 3A′; $^{+/+}$, n=2; $^{\Delta/\Delta}$, n=5), suggesting that *Nodal* expression is deregulated in $Man1^{\Delta/\Delta}$ embryos.

Man1 deficiency did not grossly affect the anteroposterior patterning of the central nervous system or axial midline, as assessed by examining the expression of cerberus-related 1 (Fig. 3D; $^{+/+}$, n=2; $^{\Delta/\Delta}$, n=2), *Otx2* and *Krox20* (Fig. 3F; $^{+/+}$, n=3; $^{\Delta/\Delta}$, n=5), *Emx2* (Fig. 3G; $^{+/+}$, n=4; $^{\Delta/\Delta}$, n=3), and sonic hedgehog (Fig. 3H; $^{+/+}$, n=5; $^{\Delta/\Delta}$, n=5).

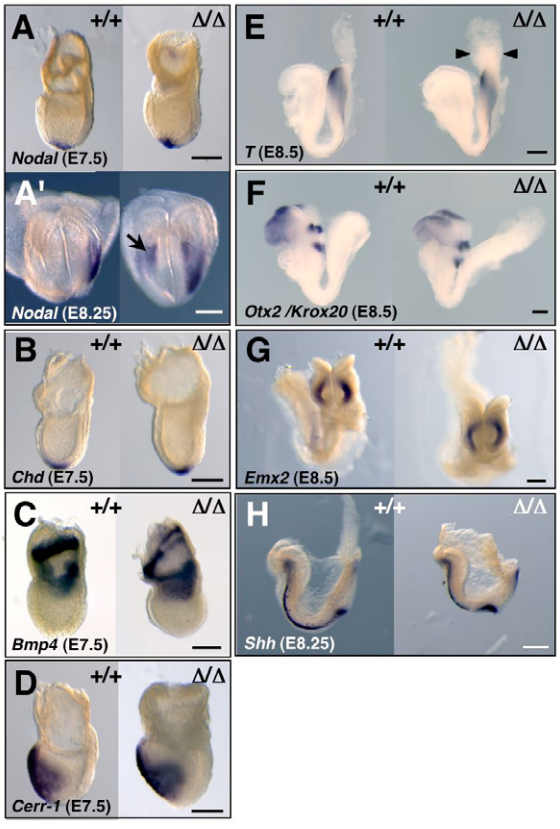

Fig. 3. *Nodal* expression is deregulated in *Man1*-deficient embryos. Whole-mount in situ hybridization for: (**A**) *Nodal* and (**B**) chordin (node), (**C**) *Bmp4* (mesoderm), (**D**) cerberus-related 1 (*Cer1*, anterior visceral endoderm), (**E**) brachyury (*T*, posterior mesoderm), (**F**) *Otx2* (forebrain) and *Krox20* (rhombomeres 3 and 5), (**G**) *Emx2* (telencephalon) and (**H**) sonic hedgehog (*Shh*, notochord) expression in wild-type and $Man1^{\Delta/\Delta}$ embryos. Anterior is towards the left, except for *Emx2* and *Nodal* at E8.25 (frontal views). Arrow indicates an ectopic expression domain of *Nodal*; arrowheads indicate an enlarged allantois. Scale bars: 200 μm.

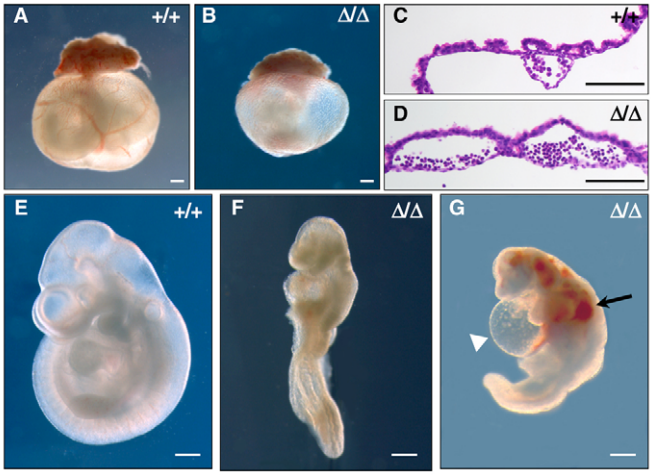

Fig. 4. Vascular defects in *Man1*$^{\Delta/\Delta}$ embryos. Gross morphology of the yolk sac (**A**,**B**) and embryo proper (**E-G**) of wild-type and *Man1*$^{\Delta/\Delta}$ embryos at E10.0. (**C**,**D**) Histological analysis of E10.0 yolk sac of wild-type and *Man1*$^{\Delta/\Delta}$ embryos. (G) Arrow indicates clumps of blood cells; white arrowhead indicates an enlarged pericardium. Scale bars: 400 μm in A,B,E-G; 100 μm in C,D.

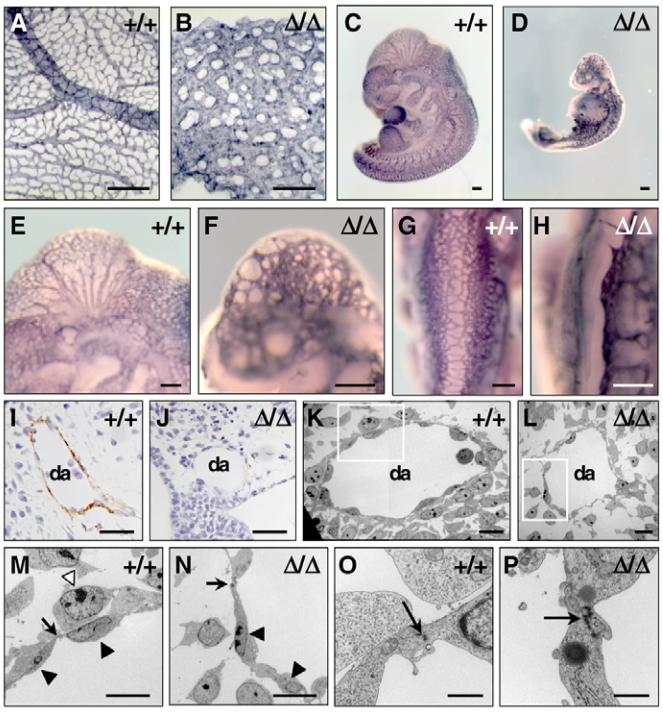

Fig. 5. *Man1*$^{\Delta/\Delta}$ embryos exhibit defective vascular remodeling. (**A-H**) Whole-mount immunostaining with an antibody to PECAM1. (A,B) The yolk sac and (C,D) embryo proper at E10.0. Closer views of blood vessels in the head region (E,F) and intersomitic vessels (G,H) of the embryos shown in C and D, respectively. (**I**,**J**) Immunohistochemical staining for smooth muscle α-actin in transverse sections of E10.0 embryos of wild-type and mutant embryos. (**K-P**) Electron microscopic analysis of the perivascular walls. (M,N) Higher magnification images of the insets in K and L, respectively. White arrowhead indicates a mural cell; black arrowheads indicate endothelial cells; arrows indicate tight junctions. (O,P) Higher-magnification views of the tight junction between endothelial cells in M and N. da, dorsal aorta. Scale bars: 200 μm in A-H; 20 μm in I,J; 10 μm in K-N; 1.0 μm in O,P.

Angiogenesis defects in *Man1* mutant embryos

At E10.0, *Man1*$^{\Delta/\Delta}$ embryos were recognizable by their smaller and pale yolk sacs (Fig. 4A,B). Histological analysis of wild-type and mutant yolk sacs revealed that the yolk sac vasculature was formed in the mutants but appeared highly dilated (Fig. 4C,D). Some mutant embryos died in the middle of turning (Fig. 4F), and others showed clumps of red blood cells and an enlarged pericardium (Fig. 4G), suggesting that vascular permeability and intracardiac pressure may have been elevated in the mutants.

Vascular defects in *Man1*$^{\Delta/\Delta}$ embryos were confirmed by whole-mount immunostaining with an antibody to platelet endothelial cell adhesion molecule 1 (Pecam1), which specifically detects endothelial cells. In the yolk sac of the wild-type embryo at E10.0, major blood vessels and a well-branched capillary network were present (Fig. 5A). By contrast, the yolk sac of the mutant embryo at E10.0 displayed a primary capillary plexus but no branching from pre-existing vessels (Fig. 5B). No significant difference in endothelial cell proliferation was observed between wild-type and mutant yolk sacs (data not shown). Moreover, in the wild-type embryo proper, well-developed and defined capillary networks were apparent in the head and intersomitic regions (Fig. 5C,E,G), whereas the fine capillary network in the cranial, branchial, cardiac and intersomitic regions of mutant embryos was absent (Fig. 5D,F,H). These data imply that endothelial cell differentiation occurred normally in *Man1*$^{\Delta/\Delta}$ embryos, but that vascular remodeling to build a mature vascular network was severely perturbed.

Interactions between endothelial cells and mural cells (pericytes and VSMCs) are essential for vascular development (Armulik et al., 2005; Carmeliet, 2000). To determine whether differentiation or recruitment of VSMCs is affected in mutant embryos, we examined the expression of smooth muscle α-actin, a marker for VSMC differentiation, by immunohistochemistry. In E10.0 wild-type embryos, the dorsal aorta was surrounded by VSMCs (Fig. 5I). However, in E10.0 mutant embryos, smooth muscle α-actin expression was barely detected around the dorsal aorta (Fig. 5J), although its expression was detected in other tissues, including the heart (data not shown). Electron microscopic analysis supported the results of immunohistochemistry (Fig. 5K-P); in wild-type embryos, endothelial cells in the dorsal aorta were surrounded by mural cells and directly in contact with them (Fig. 5K,M), whereas those in mutant embryos were not supported by mural cells, resulting in a collapsed dorsal aorta (Fig. 5L,N). Tight junctions between endothelial cells were formed in both wild-type and *Man1*$^{\Delta/\Delta}$ embryos (Fig. 5O,P). These results indicate that mural cells were differentiated normally, but their recruitment to the vascular wall was severely impaired in *Man1*$^{\Delta/\Delta}$ embryos.

The Smad2/3 pathway is abnormally activated in *Man1*$^{\Delta/\Delta}$ embryos

Null mutants of central components of the Tgfβ pathway demonstrate early embryonic death with growth retardation at about E10.0, defects in vascular development, and abnormal VMSC recruitment (Chang et al., 2002; Goumans et al., 2003). As such, there is a remarkable correlation with the defects observed in *Man1*$^{\Delta/\Delta}$ embryos, consistent with the idea that Man1 is required for manifestation of the Tgfβ signal transduction effect. Thus, we examined the activation status of the Smad1/5 and Smad2/3 pathways using a cellular resolution assay by immunohistochemistry with antibodies to phospho-Smad1/5/8 and phospho-Smad2/3. Compared

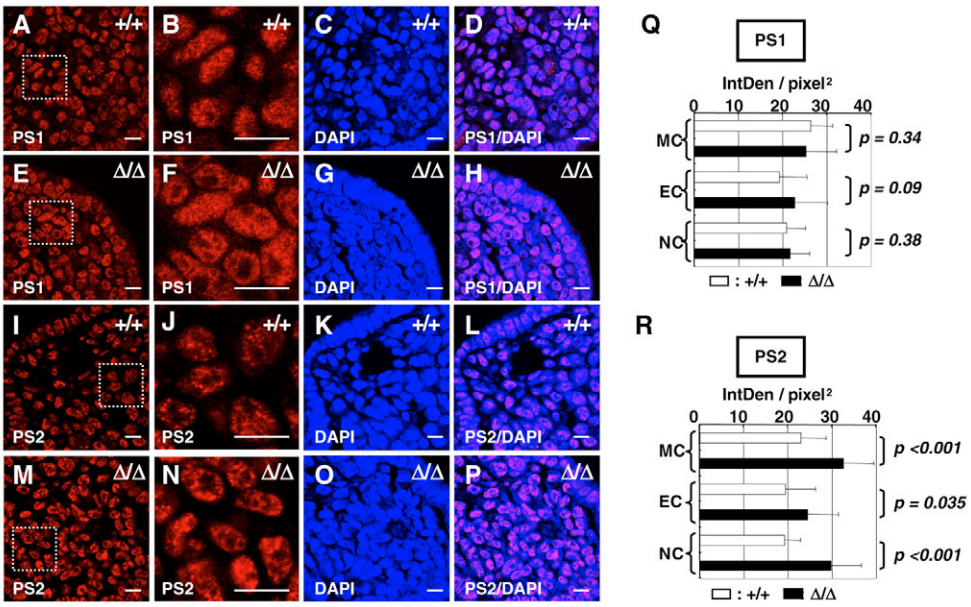

Fig. 6. Augmentation of the Smad2/3 pathway in *Man1*-deficient embryos. (**A-P**) Confocal microscopic analysis of the branchial regions of wild-type and mutant embryos at E9.5 for phospho-Smad1 (PS1) and phospho-Smad2 (PS2). Nuclei were visualized with DAPI. All pictures were recorded under the same conditions and quantified without any modifications. (B,F,J,N) Higher magnification views of the mesenchymal cells in A,E,I,M. (**Q**,**R**) For phospho-Smads quantitation, mesenchymal cells (MC, $^{+/+}$, *n*=~50; $^{\Delta/\Delta}$, *n*=~100), endothelial cells (EC, $^{+/+}$, *n*=~20; $^{\Delta/\Delta}$, *n*=~20) and neural cells (NC, $^{+/+}$, *n*=~50; $^{\Delta/\Delta}$, *n*=~50) were randomly picked up, and the intensities of PS1, PS2 and DAPI-positive areas were quantified using the NIH Image-J software. Quantitative results are expressed as integrated density (IntDen)/pixel^2 at the mean±standard deviations. Statistical differences were determined using the Student's *t*-test and the *p* values are indicated. The difference in the PS1 calculation (*P*>0.05) between the wild-type and mutant embryos was not significant.

with wild-type embryos, the intensity of nuclear phospho-Smad2 was significantly elevated in mesenchymal, endothelial, and neural cells of *Man1*$^{\Delta/\Delta}$ embryos (Fig. 6I-P, Fig. S3). Quantitative analysis revealed that accumulation of phospho-Smad2 was significantly increased in these cells in the mutants (Fig. 6R). By contrast, the difference in the intensity of phospho-Smad1 between wild-type and mutant embryos was not significant in all cell types examined (Fig. 6A-H,Q, see Fig. S2 in the supplementary material).

Augmentation of the Smad2/3 pathway was confirmed by analyzing the expression levels of its downstream targets by RT-PCR (Fig. 7A). In *Man1*$^{\Delta/\Delta}$ embryos, the expression level of *Id1*, a specific downstream target for the Smad1/5 pathway in endothelial cells (Goumans et al., 2002; Ota et al., 2002), was comparable with that in wild-type and heterozygous embryos. By contrast, the expression levels of plasminogen activator inhibitor 1 (*PAI-1*; *Serpine1* – Mouse Genome Informatics) and fibronectin 1, both of which are specific downstream targets for the Smad2/3 pathway in endothelial cells, were significantly upregulated. The expression of Smad7, which is a downstream target for both the Smad1/5 and Smad2/3 pathways, was unchanged in *Man1*$^{\Delta/\Delta}$ embryos. We obtained similar results in embryos from another cross (see Fig. S3 in the supplementary material). Notably, the expression level of *Tgfb1* was also elevated in the mutants.

Tgfβ1 strongly stimulates synthesis of extracellular matrix (ECM) and deposition of ECM inhibits vascular remodeling (Ignotz et al., 1987; Pepper, 1997). In line with the elevation of *Tgfb1* expression and the augmentation of the Smad2/3 signaling, the expression of fibronectin 1 was increased in *Man1*$^{\Delta/\Delta}$ embryos (Fig. 7A). This was further supported by western blots, where fibronectin synthesis was highly elevated (Fig. 7B), and by immunofluorescence analyses, where fibronectin was strongly deposited in *Man1*$^{\Delta/\Delta}$ embryos and yolk sacs (Fig. 7C-H). Occasionally, fibronectin deposition was extremely prominent around endothelial cells (Fig. 7D). These results suggest that abnormal activation of Smad2/3 signaling leads to aberrant deposition of ECM to inhibit migration of endothelial cells.

Man1 is required for cell survival and normal nuclear morphology

Because NE proteins are implicated in cell proliferation and apoptosis (Cohen et al., 2001; Gruenbaum et al., 2005), we examined these processes in *Man1*$^{\Delta/\Delta}$ embryos. We first analyzed cell proliferation in *Man1*$^{\Delta/\Delta}$ embryos using immunohistochemistry with an antibody against phospho-histone H3, a marker for cells in mitotic prophase. As shown in Fig. 8A,B, the number of phospho-histone H3-positive nuclei was not significantly different in wild-type and mutant embryos at the 17-somite stage, indicating that cell proliferation was normal in the mutants. Consistent with this, the expression of cyclin-dependent kinase inhibitor 1A (*Cdkn1a* or *p21*), a cyclin-dependent kinase inhibitor and mediator of the cellular growth arrest program of the Tgfβ pathway, was unchanged in *Man1*$^{\Delta/\Delta}$ embryos (Fig. 7A). By contrast, immunohistochemistry with antibodies against activated caspase 3 and single-strand DNA (ssDNA, a marker for DNA fragmentation during programmed cell death) revealed massive apoptosis in *Man1*$^{\Delta/\Delta}$ embryos (Fig. 8D,F), especially in mesenchymal tissues where *Man1* is strongly expressed (Fig. 2P). Electron microscopic analysis clarified that the mesenchymal cells in the mutants shrunk and their nuclei were condensed and fragmented, which are the typical characteristics of apoptotic cells (Fig. 8J). Wild-type embryos had few apoptotic cells (Fig. 7C,E). Notably, apoptotic cells were seldom detected in other tissues even in *Man1*$^{\Delta/\Delta}$ embryos. These results suggest that Man1 is essential for cell survival, but the degree of cell death is dependent on the different sensitivity to the loss of Man1 between cells.

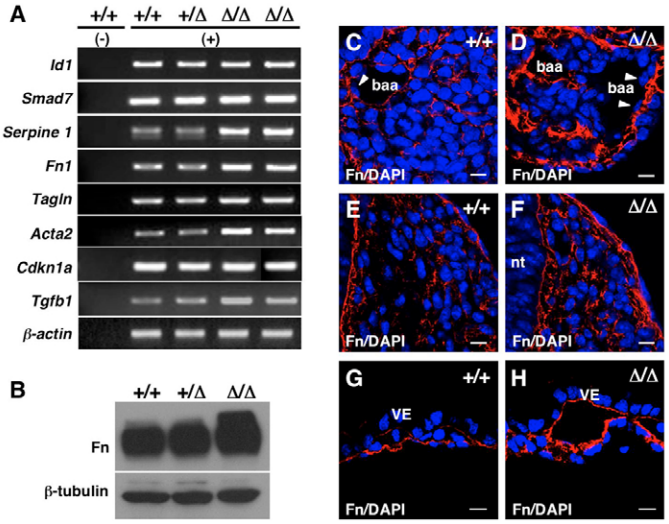

Fig. 7. Abnormal fibronectin (Fn1) deposition in *Man1*-deficient embryos. (**A**) RT-PCR analyses of whole embryos at E9.5 for the expression of downstream targets of the Smad1/5 and Smad2/3 pathways. (**B**) Western blot of whole embryos at E9.5 for fibronectin. β-Tubulin was used as a loading control. (**C-H**) Immunofluorescence analysis of the branchial arch (C,D) and trunk regions (E,F) at E9.5, and yolk sacs (G,H) at E10.0 for fibronectin. baa, branchial arch artery; nt, neural tube; VE, visceral endoderm. Arrowheads indicate endothelial cells. Scale bars: 10 μm.

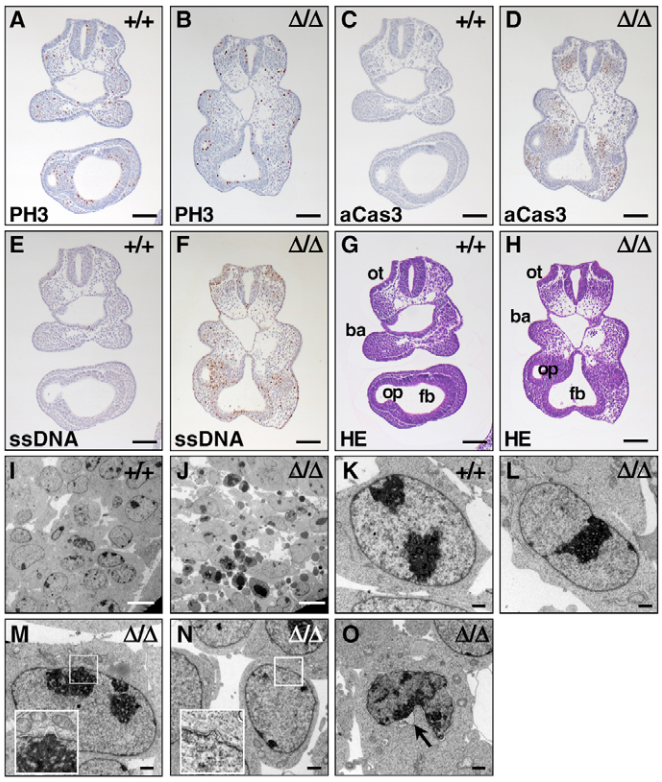

Fig. 8. Man1 is required for cell survival and normal nuclear morphology. Immunostaining on serial paraffin-embedded sections from wild-type and mutant embryos at the 17-somite stage with antibodies to phospho-histone H3 (PH3; **A**,**B**), activated caspase 3 (aCas3; **C**,**D**) and single-strand DNA (ssDNA; **E**,**F**). (**G**,**H**) Hematoxylin-Eosin staining as a reference. ot, otic vesicle; ba, first branchial arch; op, optic vesicle; fb, forebrain vesicle. (**I-O**) Transmission electron microscopy of wild-type (I,K) and *Man1*$^{\Delta/\Delta}$ (J,L-O) embryos at E9.5. (I,J) The mesenchyme in the branchial region. (K-O) The nuclear shapes of wild-type and *Man1*$^{\Delta/\Delta}$ mesenchymal cells. The insets in M and N show herniated nuclei. Arrow in O indicates an expanded perinuclear space. Scale bars: 100 μm in A-H; 10 μm in I,J; 1.0 μm in K-O.

The INM proteins bind to nuclear lamins, which are essential for maintaining nuclear shape (Gruenbaum et al., 2005); emerin, an INM protein, is required for normal nuclear shape (Lammerding et al., 2005). We next investigated whether the loss of Man1 affects the nuclear morphology by electron microscopy (Fig. 8K-O). The outlines of wild-type mesenchymal nuclei were tense and smooth, whereas the most of mutant mesenchymal nuclei were irregularly shaped, although continuity of their NE was apparently intact. At higher magnification, we found mesenchymal cells with herniated nuclei (Fig. 8M,N) and those with an expanded perinuclear space (Fig. 8O) at low frequency (~1%) in the *Man1*$^{\Delta/\Delta}$ embryos.

DISCUSSION

In our previous study of *Xenopus* embryos (Osada et al., 2003), we have proposed that XMAN1 is a novel type of negative regulator for Smad signaling. A similar hypothesis has also been proposed by four other groups (Hellemans et al., 2004; Lin et al., 2005; Pan et al., 2005; Raju et al., 2003). We have verified this hypothesis in vivo by analyzing *Man1*-deficient mice lacking the Smad-interacting domain. We have found that *Man1*$^{\Delta/\Delta}$ embryos died during embryonic development because of defects in vascular remodeling. We have demonstrated that abnormal deposition of ECM caused by the augmented Smad2/3 pathway and the disrupted intercellular communication between endothelial and mural cells underlie the perturbed vascular remodeling in *Man1*$^{\Delta/\Delta}$ embryos. Our results have shed light on the importance of Man1 in fine-tuning the activity of Tgfβ signaling during angiogenesis.

Man1 acts as a Smad regulator in angiogenesis

The Man1-βgeo fusion generated in *Man1*$^{\Delta/\Delta}$ embryo contained the N-terminal LEM domain and the first transmembrane domain, both of which are necessary and sufficient for targeting Man1 to the INM in mammalian cells (Wu et al., 2002), but lacked the C-terminal Smad-interacting domain. Thus, it is likely that the phenotypes observed in the mutants are caused by abnormal Smad regulation at the INM.

We suspect that deregulation of the Smad2/3 pathway is fundamental to the defects in vascular remodeling in *Man1*$^{\Delta/\Delta}$ embryos. We have demonstrated abnormal activation of the Smad2/3 pathway in *Man1*$^{\Delta/\Delta}$ embryos by immunofluorescence microscopy (Fig. 6, see Fig. S2 in the supplementary material), where nuclear accumulation of phospho-Smad2 is increased, and by RT-PCR (Fig. 7A), where the expression of its downstream targets is upregulated. Importantly, the expression of *Tgfb1* is elevated in *Man1*$^{\Delta/\Delta}$ embryos. The increased accumulation of nuclear Smad2 in the mutants may lead to the activation of *Tgfb1* promoter, resulting in Tgfβ1 autoinduction (Kim et al., 1989). Tgfβ1 stimulates the synthesis of fibronectin (Ignotz et al., 1987), which inhibits proliferation and migration of endothelial cells, impairing vascular remodeling (Pepper, 1997). We have shown that the expression of fibronectin is upregulated in *Man1*$^{\Delta/\Delta}$ embryos at the mRNA and protein levels (Fig. 7). In addition, the expression level of *Serpine1* is also elevated in mutant embryos. *Serpine1* is a potent inhibitor of endothelial cell migration in vitro (Stefansson

and Lawrence, 1996) and angiogenesis in vivo (Stefansson et al., 2001). Therefore, abnormal deposition of ECM caused by elevated Smad2/3 signaling could underlie the defects in vascular remodeling in *Man1*$^{\Delta/\Delta}$ embryos.

Our quantitative analyses of phospho-Smads have revealed that Smad2/3 signaling is preferentially activated in endothelial cells of *Man1*$^{\Delta/\Delta}$ embryos (Fig. 6R). Tgfβ1 can stimulate two Smad pathways in endothelial cells – the canonical Alk5-Smad2/3 pathway and the Alk1-Smad1/5 pathway (Goumans et al., 2002; Oh et al., 2000). It has been proposed that Alk1-Smad1/5 signaling promotes endothelial cell proliferation and migration and Alk5-Smad2/3 signaling inhibits them (Goumans et al., 2002). Tgfβ and activin also inhibit proliferation and sheet formation of ES cell-derived endothelial cells, probably by activating the Smad2/3 pathway (Watabe et al., 2003). Although an opposite model on the roles of the Alk1 and Alk5 pathways during angiogenesis has been proposed (Lamouille et al., 2002; Oh et al., 2000; Seki et al., 2003), the balance between the two pathways in endothelial cells appears to be crucial in determining the activation state of the endothelium. In *Man1*$^{\Delta/\Delta}$ embryos at E9.5, the expression of specific targets of the Smad2/3 pathway (*Serpine1* and *Fn1*) was significantly elevated (Fig. 7A), whereas that of *Id1*, a specific target for the Smad1/5 pathway, was unchanged, suggesting that the balance between these two pathways was disrupted in mutant endothelial cells.

It has been proposed that interactions between endothelial and mural cells in the blood vessel wall play an important role in the regulation of vascular remodeling (Armulik et al., 2005). In Fig. 5I-N, we have clearly shown that the recruitment of mural cells to the vascular wall was severely impaired in *Man1*$^{\Delta/\Delta}$ embryos. Because mural cells are generally thought to be mesenchymal origin, we speculated that the mesenchymal apoptosis observed in E9.5 *Man1*$^{\Delta/\Delta}$ embryos (Fig. 8D,E) led to the decreased numbers of VSMCs. However, we detected the elevated expression of trangelin (*Tagln*) and *Acta2* (Fig. 7A) and accumulation of SMA-positive cells around the heart in the mutants (data not shown), suggesting that proliferation and differentiation of VSMCs was normal. The activated Tgfβ1-Smad2/3 signaling, which plays an important role in VSMC development, may result in the elevation of these markers. Thus, VSMC migration rather than proliferation and differentiation may be affected in the mutants. The abnormal deposition of fibronectin around blood vessels observed in *Man1*$^{\Delta/\Delta}$ embryos would be also associated with the inhibition of VMSC migration.

Man1 in cell survival and nuclear integrity

Man1 is highly expressed in the head mesenchyme (Fig. 2P), where massive apoptosis was observed in *Man1*$^{\Delta/\Delta}$ embryos. Loss of Ce-MAN1 in *C. elegans* and siRNA interference of human MAN1 in cultured cells also induce apoptosis (Liu et al., 2003; Pan et al., 2005). Although these results suggest that the mesenchymal apoptosis in *Man1*$^{\Delta/\Delta}$ embryos is probably a direct consequence of the loss of Man1, the elevated *Tgfb1* expression may be implicated in initiation or deterioration of the apoptotic processes. We have clarified that most of the apoptotic cells in the mesenchyme are caspase 3-dependent (Fig. 7D), consistent with the observation that caspase 3 is activated during Tgfβ1-induced apoptosis in many types of cultured cells (Schuster and Krieglstein, 2002). In addition, several lines of evidence have shown that Smad3 is an important mediator of Tgfβ1-induced apoptosis (Kim et al., 2002; Yamamura et al., 2000; Yanagisawa et al., 1998). Thus, the elevated Smad2/3 pathway in the mutants may also be involved in the Tgfβ1-induced caspase 3-dependent apoptosis.

Nuclear lamins and the INM proteins play a key role in maintaining nuclear morphology (Burke and Stewart, 2002). We observed nuclear anomalies, especially in mesenchymal cells of *Man1*$^{\Delta/\Delta}$ mutants (Fig. 8L-O), although we seldom found the cells with discontinuous NE. It remains to be elucidated whether the nuclear abnormalities in the mutants were caused by the abnormal regulation of Smad signaling at the INM, or by the presence of structurally aberrant Man1 with the long C-terminal tail of βgeo, and they are associated with the increased mesenchymal apoptosis. Emerin-deficient MEFs show abnormal nuclear shape and increased apoptosis, but impaired mechanotransduction rather than nuclear fragility induces their apoptosis (Lammerding et al., 2005).

Man1 in axis formation

Nodal expression in the node and left LPM during early embryogenesis plays a crucial role in determining the left-right axis of the embryo (Hamada et al., 2002; Lowe et al., 1996). In *Man1*$^{\Delta/\Delta}$ embryos, initiation of *Nodal* expression and gastrulation occurred normally. However, asymmetric *Nodal* expression was impaired to become expressed bilaterally in mutant embryos (Fig. 3A′). It would be intriguing to examine whether Man1 is involved in establishing left-right asymmetry through the regulation of *Nodal* expression.

In *Man1*$^{\Delta/\Delta}$ embryos, the overall anteroposterior patterning of the embryo proper and the initiation of the expression of neural markers are normal (Fig. 3), which is consistent with previous data in XMAN1 morphants (Osada et al., 2003). However, in contrast to the XMAN1 morphants that show eyeless phenotypes with anterior truncations, the anterior structures are relatively normal in *Man1* mutants. Early embryonic lethality at about E10.5 in *Man1*$^{\Delta/\Delta}$ embryos prevented us from examining the role of Man1 in neural development. Generation of conditional *Man1* mutant mice would be useful for analyzing the cell- and tissue-specific roles of Man1 more precisely.

In cultured cells, depletion of human MAN1 leads to elevated responsiveness to both TGFβ and BMP (Hellemans et al., 2004; Lin et al., 2005; Pan et al., 2005). Accordingly, the sensitivity to both activin/nodal and Bmp stimulation was expected to be elevated in the setting of *Man1* deficiency. The mechanism by which the Smad2/3 pathway was preferentially augmented in *Man1*$^{\Delta/\Delta}$ embryos is currently unknown. Intracellular antagonism between Bmp4 and activin signaling through competition for a limited pool of Smad4 has been proposed (Candia et al., 1997). Thus, it is possible that the Smad2/3 pathway activated by continuous Tgfβ1 stimulation consumed more Smad4 than the Smad1/5 pathway, leading to the dominance of the Smad2/3 pathway in *Man1* mutants.

We did not detect overt morphological defects caused by the abnormal activation of the Bmp-Smad1/5 pathway in *Man1*$^{\Delta/\Delta}$ embryos, aside from the fact that the allantois was enlarged in the mutant embryos (Fig. 3E). Bmp signaling plays a crucial role in the development of the allantois (Fujiwara et al., 2001). It would be important to examine the development of tissues/cell population where the involvement of the Bmp-Smad1/5 pathway is implicated, such as the formation of the heart and primordial germ cells, and the dorsoventral patterning of the neural tube (Hogan, 1996).

We thank Dr N. Osumi for instructions on mouse dissection; Drs Y. Suda, H. Sasaki, A. Shimono and R. Behringer for mouse in situ probes; Dr H. Worman for the MAN1 expression plasmid; Drs K. Hamada and M. Nakaya for the experimental protocols; Drs N. Inagaki, K. Hasegawa and N. Ban for the reagents; Drs M. Shibuya and Y. Sakurai for the PCR primer sequences; Dr T. Momoi for the antibody to activated caspase 3; Drs C. Wright, T. Watabe and K. Kawamura for helpful suggestions and discussions. We also thank S. Hatazawa, H. Watanabe and S. Chida for technical assistance; and A. Takahashi for assistance in performing the in situ hybridization. This work was

supported by Grants-in-Aid for Scientific Research from the Ministry of Education, Culture, Sports, Science and Technology of Japan; by a grant from the Kanae Foundation for Life and Socio-Medical Science to S.O.; and by an NHLBI-funded Program in Genomics Applications ['BayGenomics' (HL66621, HL66600 and HL66590)].

Supplementary material

Supplementary material for this article is available at http://dev.biologists.org/cgi/content/full/133/19/3919/DC1

References

Armulik, A., Abramsson, A. and Betsholtz, C. (2005). Endothelial/pericyte interactions. *Circ. Res.* **97**, 512-523.

Burke, B. and Stewart, C. L. (2002). Life at the edge: the nuclear envelope and human disease. *Nat. Rev. Mol. Cell Biol.* **3**, 575-585.

Candia, A. F., Watabe, T., Hawley, S. H., Onichtchouk, D., Zhang, Y., Derynck, R., Niehrs, C. and Cho, K. W. (1997). Cellular interpretation of multiple TGF-β signals: intracellular antagonism between activin/BVg1 and BMP-2/4 signaling mediated by Smads. *Development* **124**, 4467-4480.

Carmeliet, P. (2000). Mechanisms of angiogenesis and arteriogenesis. *Nat. Med.* **6**, 389-395.

Chang, H., Brown, C. W. and Matzuk, M. M. (2002). Genetic analysis of the mammalian transforming growth factor-β superfamily. *Endocr. Rev.* **23**, 787-823.

Cohen, M., Lee, K. K., Wilson, K. L. and Gruenbaum, Y. (2001). Transcriptional repression, apoptosis, human disease and the functional evolution of the nuclear lamina. *Trends Biochem. Sci.* **26**, 41-47.

Fujiwara, T., Dunn, N. R. and Hogan, B. L. (2001). Bone morphogenetic protein 4 in the extraembryonic mesoderm is required for allantois development and the localization and survival of primordial germ cells in the mouse. *Proc. Natl. Acad. Sci. USA* **98**, 13739-13744.

Giro, M. G., Duvic, M., Smith, L. T., Kennedy, R., Rapini, R., Arnett, F. C. and Davidson, J. M. (1992). Buschke-Ollendorff syndrome associated with elevated elastin production by affected skin fibroblasts in culture. *J. Invest. Dermatol.* **99**, 129-137.

Goumans, M. J., Valdimarsdottir, G., Itoh, S., Rosendahl, A., Sideras, P. and ten Dijke, P. (2002). Balancing the activation state of the endothelium via two distinct TGF-β type I receptors. *EMBO J.* **21**, 1743-1753.

Goumans, M. J., Lebrin, F. and Valdimarsdottir, G. (2003). Controlling the angiogenic switch: a balance between two distinct TGF-β receptor signaling pathways. *Trends Cardiovasc. Med.* **13**, 301-307.

Gruenbaum, Y., Margalit, A., Goldman, R. D., Shumaker, D. K. and Wilson, K. L. (2005). The nuclear lamina comes of age. *Nat. Rev. Mol. Cell Biol.* **6**, 21-31.

Hamada, H., Meno, C., Watanabe, D. and Saijoh, Y. (2002). Establishment of vertebrate left-right asymmetry. *Nat. Rev. Genet.* **3**, 103-113.

Harland, R. (2000). Neural induction. *Curr. Opin. Genet. Dev.* **10**, 357-362.

Hellemans, J., Preobrazhenska, O., Willaert, A., Debeer, P., Verdonk, P. C., Costa, T., Janssens, K., Menten, B., Van Roy, N., Vermeulen, S. J. et al. (2004). Loss-of-function mutations in LEMD3 result in osteopoikilosis, Buschke-Ollendorff syndrome and melorheostosis. *Nat. Genet.* **36**, 1213-1218.

Hogan, B. L. (1996). Bone morphogenetic proteins: multifunctional regulators of vertebrate development. *Genes Dev.* **10**, 1580-1594.

Ignotz, R. A., Endo, T. and Massague, J. (1987). Regulation of fibronectin and type I collagen mRNA levels by transforming growth factor-β. *J. Biol. Chem.* **262**, 6443-6446.

Jones, C. M., Kuehn, M. R., Hogan, B. L., Smith, J. C. and Wright, C. V. (1995). Nodal-related signals induce axial mesoderm and dorsalize mesoderm during gastrulation. *Development* **121**, 3651-3662.

Kay, B. K. and Peng, H. B. (1991). *Xenopus Laevis: Practical uses in Cell and Molecular Biology*. San Diego: Academic Press.

Kim, B. C., Mamura, M., Choi, K. S., Calabretta, B. and Kim, S. J. (2002). Transforming growth factor β 1 induces apoptosis through cleavage of BAD in a Smad3-dependent mechanism in FaO hepatoma cells. *Mol. Cell. Biol.* **22**, 1369-1378.

Kim, S. J., Jeang, K. T., Glick, A. B., Sporn, M. B. and Roberts, A. B. (1989). Promoter sequences of the human transforming growth factor-β 1 gene responsive to transforming growth factor-β 1 autoinduction. *J. Biol. Chem.* **264**, 7041-7045.

Lammerding, J., Hsiao, J., Schulze, P. C., Kozlov, S., Stewart, C. L. and Lee, R. T. (2005). Abnormal nuclear shape and impaired mechanotransduction in emerin-deficient cells. *J. Cell Biol.* **170**, 781-791.

Lamouille, S., Mallet, C., Feige, J. J. and Bailly, S. (2002). Activin receptor-like kinase 1 is implicated in the maturation phase of angiogenesis. *Blood* **100**, 4495-4501.

Lin, F., Blake, D. L., Callebaut, I., Skerjanc, I. S., Holmer, L., McBurney, M. W., Paulin-Levasseur, M. and Worman, H. J. (2000). MAN1, an inner nuclear membrane protein that shares the LEM domain with lamina-associated polypeptide 2 and emerin. *J. Biol. Chem.* **275**, 4840-4847.

Lin, F., Morrison, J. M., Wu, W. and Worman, H. J. (2005). MAN1, an integral protein of the inner nuclear membrane, binds Smad2 and Smad3 and antagonizes transforming growth factor-β signaling. *Hum. Mol. Genet.* **14**, 437-445.

Liu, J., Lee, K. K., Segura-Totten, M., Neufeld, E., Wilson, K. L. and Gruenbaum, Y. (2003). MAN1 and emerin have overlapping function(s) essential for chromosome segregation and cell division in Caenorhabditis elegans. *Proc. Natl. Acad. Sci. USA* **100**, 4598-4603.

Lowe, L. A., Supp, D. M., Sampath, K., Yokoyama, T., Wright, C. V., Potter, S. S., Overbeek, P. and Kuehn, M. R. (1996). Conserved left-right asymmetry of nodal expression and alterations in murine situs inversus. *Nature* **381**, 158-161.

Mans, B. J., Anantharaman, V., Aravind, L. and Koonin, E. V. (2004). Comparative genomics, evolution and origins of the nuclear envelope and nuclear pore complex. *Cell Cycle* **3**, 1612-1637.

Nagy, A., Gertsenstein, M., Vintersten, K. and Behringer, R. (2003). *Manipulating the Mouse Embryo: A Laboratory Manual*. New York: Cold Spring Harbor Laboratory Press.

Nieuwkoop, P. D. and Faber, J. (1967). *Normal Table of* Xenopus laevis *(Daudin)*. Amsterdam: North Holland.

Oh, S. P., Seki, T., Goss, K. A., Imamura, T., Yi, Y., Donahoe, P. K., Li, L., Miyazono, K., ten Dijke, P., Kim, S. et al. (2000). Activin receptor-like kinase 1 modulates transforming growth factor-β 1 signaling in the regulation of angiogenesis. *Proc. Natl. Acad. Sci. USA* **97**, 2626-2631.

Osada, S.-I., Saijoh, Y., Frisch, A., Yeo, C. Y., Adachi, H., Watanabe, M., Whitman, M., Hamada, H. and Wright, C. V. (2000). Activin/nodal responsiveness and asymmetric expression of a *Xenopus* nodal-related gene converge on a FAST-regulated module in intron 1. *Development* **127**, 2503-2514.

Osada, S.-I., Ohmori, S. Y. and Taira, M. (2003). XMAN1, an inner nuclear membrane protein, antagonizes BMP signaling by interacting with Smad1 in *Xenopus* embryos. *Development* **130**, 1783-1794.

Ota, T., Fujii, M., Sugizaki, T., Ishii, M., Miyazawa, K., Aburatani, H. and Miyazono, K. (2002). Targets of transcriptional regulation by two distinct type I receptors for transforming growth factor-β in human umbilical vein endothelial cells. *J. Cell Physiol.* **193**, 299-318.

Pan, D., Estevez-Salmeron, L. D., Stroschein, S. L., Zhu, X., He, J., Zhou, S. and Luo, K. (2005). The integral inner nuclear membrane protein MAN1 physically interacts with the R-Smad proteins to repress signaling by the transforming growth factor-β superfamily of cytokines. *J. Biol. Chem.* **280**, 15992-16001.

Pepper, M. S. (1997). Transforming growth factor-β: vasculogenesis, angiogenesis, and vessel wall integrity. *Cytokine Growth Factor Rev.* **8**, 21-43.

Raju, G. P., Dimova, N., Klein, P. S. and Huang, H. C. (2003). SANE, a novel LEM domain protein, regulates bone morphogenetic protein signaling through interaction with Smad1. *J. Biol. Chem.* **278**, 428-437.

Sasai, Y., Lu, B., Steinbeisser, H., Geissert, D., Gont, L. K. and De Robertis, E. M. (1994). *Xenopus* chordin: a novel dorsalizing factor activated by organizer-specific homeobox genes. *Cell* **79**, 779-790.

Schirmer, E. C., Florens, L., Guan, T., Yates, J. R., 3rd and Gerace, L. (2003). Nuclear membrane proteins with potential disease links found by subtractive proteomics. *Science* **301**, 1380-1382.

Schuster, N. and Krieglstein, K. (2002). Mechanisms of TGF-β-mediated apoptosis. *Cell Tissue Res.* **307**, 1-14.

Seki, T., Yun, J. and Oh, S. P. (2003). Arterial endothelium-specific activin receptor-like kinase 1 expression suggests its role in arterialization and vascular remodeling. *Circ. Res.* **93**, 682-689.

Stefansson, S. and Lawrence, D. A. (1996). The serpin PAI-1 inhibits cell migration by blocking integrin alpha V β 3 binding to vitronectin. *Nature* **383**, 441-443.

Stefansson, S., Petitclerc, E., Wong, M. K., McMahon, G. A., Brooks, P. C. and Lawrence, D. A. (2001). Inhibition of angiogenesis in vivo by plasminogen activator inhibitor-1. *J. Biol. Chem.* **276**, 8135-8141.

Watabe, T., Nishihara, A., Mishima, K., Yamashita, J., Shimizu, K., Miyazawa, K., Nishikawa, S. and Miyazono, K. (2003). TGF-β receptor kinase inhibitor enhances growth and integrity of embryonic stem cell-derived endothelial cells. *J. Cell Biol.* **163**, 1303-1311.

Whitman, M. (1998). Smads and early developmental signaling by the TGFβ superfamily. *Genes Dev.* **12**, 2445-2462.

Wu, W., Lin, F. and Worman, H. J. (2002). Intracellular trafficking of MAN1, an integral protein of the nuclear envelope inner membrane. *J. Cell Sci.* **115**, 1361-1371.

Yamaguchi, T. P., Dumont, D. J., Conlon, R. A., Breitman, M. L. and Rossant, J. (1993). flk-1, an flt-related receptor tyrosine kinase is an early marker for endothelial cell precursors. *Development* **118**, 489-498.

Yamamura, Y., Hua, X., Bergelson, S. and Lodish, H. F. (2000). Critical role of Smads and AP-1 complex in transforming growth factor-β-dependent apoptosis. *J. Biol. Chem.* **275**, 36295-36302.

Yanagisawa, K., Osada, H., Masuda, A., Kondo, M., Saito, T., Yatabe, Y., Takagi, K., Takahashi, T. and Takahashi, T. (1998). Induction of apoptosis by Smad3 and down-regulation of Smad3 expression in response to TGF-β in human normal lung epithelial cells. *Oncogene* **17**, 1743-1747.

Table S1. Genotype analysis of embryos from *Man1*$^{+/\Delta}$ intercrosses

	Genotype			Total
	+/+	+/Δ	Δ/Δ	
E7.5	13	31	15	59
E8.5	7	16	10	33
E9.5	25	58	25	108
E10.0	21	30	15	66
E10.5	7	14	8	29
E11.5	6	18	5*	29
E12.5	14	9	0	33
E16.5	7	10	0	17
4W	10	22	0	32

*These embryos were partially absorbed.